

## Supporting Information for:

A long-wavelength xanthene dye for photoacoustic imaging

### Authors:

Xinqi Zhou,<sup>a</sup> Yuan Fang,<sup>b</sup> Viranga Wimalasiri,<sup>b</sup> Cliff I. Stains,<sup>b,c</sup> and Evan W. Miller<sup>a,d,e,\*</sup>

### Affiliations:

Department of <sup>a</sup>Chemistry and <sup>d</sup>Molecular & Cell Biology and <sup>e</sup>Helen Wills Neuroscience Institute. University of California, Berkeley, California 94720, United States

<sup>b</sup>Department of Chemistry and <sup>c</sup>University of Virginia Cancer Center. University of Virginia, Charlottesville, Virginia 22904, United States

\*Corresponding Author

E-mail: [evanwmiller@berkeley.edu](mailto:evanwmiller@berkeley.edu)

DOI: 10.1039/d2cc03947h

## Table of Contents

Chemical Synthesis, Purification, and Characterization.....	3
Spectroscopic Studies .....	3
General Considerations.....	3
Molar Extinction Coefficient Measurement .....	3
Fluorescence Emission Spectra and Solvent Re-absorption Correction.....	4
Quantum Yield Measurement.....	4
PA Imaging.....	4
Tissue-mimicking Phantom Recipe and Dye Loading .....	4
Data Acquisition and Processing .....	5
Supporting Tables.....	6
<b>Table S1.</b> Electrophiles screening for inserting ketone group at 10' position of KeTMR. ....	6
<b>Table S2.</b> Photophysical properties comparison among tetramethyl xanthene dyes. All parameters were measured in DPBS (pH = 7.2, with 0.5% DMSO) at room temperature.....	6
<b>Table S3.</b> Summary of absorption and emission profiles of KeTMR and KeJuR in various solvents. ....	6
<b>Table S4.</b> Comparison of KR-1, <sup>5</sup> KeTMR, and KeJuR .....	7
Supporting Figures.....	8
<b>Figure S1.</b> Structures and optical spectra of various tetramethyl xanthene dyes. ....	8

<b>Figure S2.</b>	Normalized absorbance and fluorescence spectra of KeTMR and KeJuR in various solvents.....	9
<b>Figure S3.</b>	The absorption and emission maximum of KeTMR and KeJuR in various solvents against solvent dielectric constants.....	10
<b>Figure S4.</b>	Effect of solvent properties on KeTMR and KeJuR.....	11
<b>Figure S5.</b>	KeTMR and KeJuR chemical stabilities against GSH. ....	12
<b>Figure S6.</b>	KeJuR concentration dependent PA signal.....	13
<b>Figure S7.</b>	Photostability of KeTMR and KeJuR.....	14
Detailed Synthetic Procedures .....		15
	Screening electrophiles for KeTMR synthesis: .....	15
	Synthesis of 9,9'-( <i>o</i> -tolylmethylene)bis(8-bromo-2,3,6,7-tetrahydro-1H,5H-pyrido[3,2,1- <i>ij</i> ]quinoline) .....	17
	Synthesis of KeJuR.....	18
Supporting Spectra.....		20
<b>Spectrum S1.</b>	<sup>1</sup> H NMR chart of KeTMR without I <sub>2</sub> in Chloroform- <i>d</i> . No clear product peaks could be assigned. 20	
<b>Spectrum S2.</b>	<sup>1</sup> H NMR chart of KeTMR with I <sub>2</sub> in Chloroform- <i>d</i> . ....	21
<b>Spectrum S3.</b>	EPR Spectrum of KeTMR (2 mM in Dichloromethane) with and without Iodine.....	22
<b>Spectrum S4.</b>	<sup>13</sup> C NMR chart of KeTMR with I <sub>2</sub> in Chloroform- <i>d</i> . ....	23
<b>Spectrum S5.</b>	<sup>1</sup> H NMR chart of 9,9'-( <i>o</i> -tolylmethylene)bis(8-bromo-2,3,6,7-tetrahydro-1H,5H-pyrido[3,2,1- <i>ij</i> ]quinoline)in Chloroform- <i>d</i> . ....	24
<b>Spectrum S6.</b>	<sup>13</sup> C NMR chart of 9,9'-( <i>o</i> -tolylmethylene)bis(8-bromo-2,3,6,7-tetrahydro-1H,5H-pyrido[3,2,1- <i>ij</i> ]quinoline)in Chloroform- <i>d</i> . ....	25
<b>Spectrum S7.</b>	<sup>1</sup> H NMR chart of KeJuR in Chloroform- <i>d</i> .....	26
<b>Spectrum S8.</b>	<sup>13</sup> C NMR chart of KeJuR in Chloroform- <i>d</i> .....	27

## Chemical Synthesis, Purification, and Characterization

Unless otherwise noted, reactions were performed using standard Schlenk techniques under N<sub>2</sub>. All reagents were purchased from commercial suppliers and used without further purification. Tetrahydrofuran and diethyl ether were purified with a solvent purification system (MBRAUN, SPS-5) and further dried with 3 Å molecular sieves.<sup>1</sup> Reaction progress was monitored using thin layer chromatography (TLC, silica gel, F254, 250 μm).

Products were purified by either normal phase flash chromatography using Merck silica gel 60 (230-400 mesh), or by reverse phase high performance liquid chromatography (HPLC) using a Waters 1525 Binary HPLC pump with a 2489 UV/Vis detector. Prep HPLC purification was performed with a semi-prep column (YMC-Pack ODS-A, 5 μm, 250×20 mm) using a gradient of 5 % to 95 % acetonitrile in water containing 0.1 % trifluoroacetic acid over 40 min. Final dye products were lyophilized (Labconco™ FreeZone™ 4.5L -84°C) after prep HPLC.

Low-resolution ESI Mass Spectrometry was performed with Advion CMS-S01 ESI mass spectrometer, and high-resolution mass spectrometry was recorded with Agilent 6545 Q-TOF paired with Agilent 1260 Infinity II Prime liquid chromatography (LC) system. Mass data were reported in units of m/z for [M-I]<sup>+</sup> or [M+H]<sup>+</sup>. NMR spectra were recorded on Varian VNMRS 600 MHz (echo) and data were processed with MestReNova software. Chemical shifts (δ) are expressed in parts per million (ppm) and are referenced to Chloroform-*d* (7.26 ppm for <sup>1</sup>H NMR, and 77.16 ppm for <sup>13</sup>C NMR). Coupling constants are reported as Hertz (Hz). Splitting patterns are indicated as follows: s, singlet; d, doublet; t, triplet; q, quartet; dd, doublet of doublet; td, triplet of doublets; dt, doublet of triplets; tt, triplet of triplets; ddd, doublet of doublet of doublets; tdd, triplet of doublet of doublets; q, quartet; m, multiplet. For CW-EPR measurements, 6 μL sample is loaded into 0.84 x 0.6 mm quartz capillaries (VitroCom, Mountain Lakes, NJ). EPR spectra is recorded at room temperature at X-band using a Bruker EMX spectrometer (Billerica, MA) with an ER 4123D dielectric resonator using a sweep width of 100 gauss (G), a modulation amplitude of 1 G, and 2 mW incident microwave power. Data were collected as additive averages of 10 scans.

## Spectroscopic Studies

### *General Considerations*

UV-Vis-NIR absorbance spectra were recorded with Jasco V-780. UV-Vis band width was set to 1 nm, and NIR band width was set to 2 nm. Response time for both UV/Vis and NIR was 0.96 s. Scanning interval was 1 nm and scan speed was 400 nm/min (continuous mode). All absorbance assays were conducted in a 3.5 mL quartz cuvettes with 1 cm optical path length.

Fluorescence spectra were recorded with Fluorolog-QM (Horiba). The fluorometer was equipped with a 75 W Xenon Arc lamp with PowerArc™ lamp housing (OB-75X), photomultiplier tube (920 PMT) detector, liquid nitrogen cooled indium gallium arsenide (InGaAs) detector (DSS-IGA020L/100KHZ) and related power suppliers and controllers. The sample holder could be switched to an integrating sphere (K-Sphere) for measuring absolute quantum efficiencies. The excitation light source could be switched to a tunable white laser (SuperK Extreme EXU-6 PP), and PMT detector was connected to high throughput Time-Correlated Single Photon Counting (TCSPC) controller (Delta Hub, Horiba) to allow for lifetime-based measurements.

DPBS (Dulbecco's phosphate buffered saline)<sup>2</sup> was from ThermoFisher (14190144), and contained (in mM): KCl, 2.67; KH<sub>2</sub>PO<sub>4</sub>, 1.47; NaCl, 137.93, Na<sub>2</sub>HPO<sub>4</sub>, 8.06.

### *Molar Extinction Coefficient Measurement*

Dye stock solutions (typically 10 mM) were made by dissolving the lyophilized dye powder in DMSO. Increasing concentrations of samples (2, 4, 6, 8, 10 μM) as well as blank (DPBS with 0.5% DMSO) were made and their absorbances were measured. Molar extinction coefficient was then determined by a linear fit of the absorbance versus sample concentrations according to the Beer-Lambert law.

### *Fluorescence Emission Spectra and Solvent Re-absorption Correction*

Dye solutions in various solvents were made by either directly dissolving the lyophilized powder (organic solvents) or by dissolving the dye stock in DMSO (aqueous solvents). In both cases, the absorbance maximum was kept below 0.1 before measuring the emission spectra to avoid dye re-absorption.

In order to obtain the solvent-reabsorption correction factor, the transmittances of various solvents with 1 cm optical path length were recorded (600 nm – 1400 nm) first. As there should be no absorption occurring at 600 nm for all the solvents, the raw transmittances data obtained above were then adjusted to 1 at 600 nm through spectral shifting. This gave the solvent re-absorption correction factor with 1 cm optical path  $T_{1\text{ cm}}$ . However, when the fluorescence was measured, the emissive signal was detected 90 degree from the incident light, meaning the emission light travelled only 0.5 cm within the solvents. It is therefore necessary to calculate the transmittances for 0.5 cm optical path to avoid over-correction. Since  $A_{0.5\text{ cm}} = 0.5 \times A_{1\text{ cm}}$ , and  $A = -\log_{10}T$ , then  $T_{0.5\text{ cm}} = T_{1\text{ cm}}^{0.5}$ . Therefore, the following equation gave the true emission after correction:

$$Em_{\text{ture}} = Em_{\text{raw}} / T_{0.5\text{ cm}} = \frac{Em_{\text{raw}}}{\sqrt{T_{1\text{ cm}}}}$$

### *Quantum Yield Measurement*

Absolute quantum yield measurement with integrating sphere. Following previously reported protocol,<sup>3</sup> which involved solvent re-absorption correction and dye re-absorption / re-emitting correction after getting the raw quantum efficiency.

Relative Quantum Yield measurement. Relative fluorescence quantum yield was determined by the following equation:

$$\Phi_x = (\Phi_{\text{ST}} \times A_{\text{ST}} \times F_x \times \eta_x^2) / (A_x \times F_{\text{ST}} \times \eta_{\text{ST}}^2)$$

$\Phi$  is the quantum yield;  $A$  is the absorbance at the excitation wavelength ( $A$  was kept at  $\leq 0.1$  during fluorescence measurements to avoid self-quenching),  $F$  is the fluorescence intensity at the excitation wavelength;  $\eta$  is the refractive index of the solvent. The subscripts  $\text{ST}$  and  $x$  refer to the standard and unknown respectively.

### **PA Imaging**

#### *Tissue-mimicking Phantom Recipe and Dye Loading*

Adapted from previously reported protocols:<sup>4</sup> 6 g agarose, 3 mL 2 % milk (freshly made from powder milk 0.5 g in 25 mL water), and 117 mL deionized water were mixed in a 250 mL beaker. Upon heating with a microwave (Sunbeam, 60 % power), the fully dissolved gel was transferred to a mold by drilling holes of a 50 mL centrifuge tube and a FEP (0.08'' diameter, 10 cm long) tube through the hole for loading samples. This solution was sufficient to make 2 phantoms. The gel was allowed to solidify in the mold for at least 3 h before it was taken out and cut to fit the PA imaging holder. FEP tube was sealed on one end with glue gun and  $\sim 1$  mL sample solution was injected through the seal via a 25 G BD needle to avoid any bubbles in the tube. Upon filling the tube with sample solution, both ends of the tube were sealed with glue gun and the phantom was ready for imaging.

For phantoms with 60% milk: 6 g agarose, 3 mL 60 % milk (freshly made from powder milk 15 g in 25 mL water), and 117 mL deionized water were mixed in a 250 mL beaker. All the other procedures were identical as the 2 % milk mentioned above.

For dual-color imaging experiments, two holes were drilled so that two FEP tube could be inserted in one phantom. The distance between the center of the two holes and the detection units after placing the phantom into the sample holder was kept as similar as possible to allow for fair data acquisition and comparison.

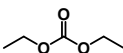
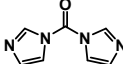
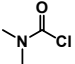
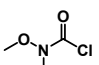
For imaging in blood samples: Dyes (in DMSO stock) were pre-mixed with defibrinated sheep blood (Thermo Scientific, R54020) and loaded into the FEP tubes through a 25 G BD needle, similar to the procedures of loading dye to buffer solution mentioned above. Both ends of the tube were sealed with glue gun before imaging.

#### *Data Acquisition and Processing*

PA data was acquired on iThera Medical inVision 256-TF, and data were processed with viewMSOT 4.0.2.0 software. Model based (MB) reconstruction method was used for data analysis. For spectral unmixing, plots of extinction coefficient vs. wavelengths for KeJuR and ICG were imported into the viewMSOT software. Along with these two plots, water, oxyhaemoglobin, deoxyhemoglobin, blank phantom profiles (pre-installed in the software) were selected and linear regression method was used to unmix the signal.

## Supporting Tables

**Table S1.** Electrophiles screening for inserting ketone group at 10' position of KeTMR.

Electrophile Name	Electrophile Structure	Yield
Diethyl carbonate		< 10 %
Carbonyldiimidazole		No Product
Dimethylcarbonyl chloride		70 %
<i>N</i> -methoxy- <i>N</i> -methylcarbonyl chloride		83 %

**Table S2.** Photophysical properties comparison among tetramethyl xanthene dyes. All parameters were measured in DPBS (pH = 7.2, with 0.5% DMSO) at room temperature.

Dye	10' Functional Group	Abs (nm)	Abs FWHM (cm <sup>-1</sup> )	Em (nm)	Em FWHM (cm <sup>-1</sup> )	Stokes Shift (nm) / (cm <sup>-1</sup> )	$\epsilon$ (M <sup>-1</sup> ·cm <sup>-1</sup> )	$\phi$ (%)	$\epsilon \times \phi$
TMR	O	550	1066	568	1011	18 / 576	74500	31	23095
RF <sub>620</sub>	B(OH) <sub>2</sub>	620	922	636	929	16 / 406	109000	36	39240
SiMe <sub>2</sub> R	SiMe <sub>2</sub>	646	894	664	852	18 / 420	125000	32	40000
NR <sub>700</sub>	P(O)OEt	700	942	722	878	22 / 435	71000	11	7810
KeTMR	C(O)	856	2434	1006	1857	150 / 1742	26880	0.013	3.5

**Table S3.** Summary of absorption and emission profiles of KeTMR and KeJuR in various solvents.

Solvents	KeTMR					KeJuR				
	Abs Max (nm)	Abs FWHM (cm <sup>-1</sup> )	Em Max (nm)	Em FWHM (cm <sup>-1</sup> )	Stokes shift (cm <sup>-1</sup> )	Abs Max (nm)	Abs FWHM (cm <sup>-1</sup> )	Em Max (nm)	Em FWHM (cm <sup>-1</sup> )	Stokes shift (cm <sup>-1</sup> )
Toluene	789	2558	837	1373	727	832	1773	876	995	604
DCM	846	1015	882	1026	482	856	923	883	996	357
Chloroform	845	1947	882	1174	496	850	986	882	1044	427
DMSO	864	2192	937	1158	902	860	1685	924	1096	805
DMF	844	2243	921	1214	991	858	1542	918	1082	762
Acetone	847	2029	905	1132	757	848	1317	894	1071	607
Acetonitrile	844	2021	901	1203	750	848	1263	900	1124	681
<i>n</i> -BuOH	848	2314	877	1466	390	850	1092	878	1099	375
IPA	847	2070	878	1501	417	849	1082	877	1208	376
EtOH	843	1995	907	1629	837	852	1144	877	1339	335
MeOH	840	2046	923	1801	1071	847	1272	905	1571	757
D <sub>2</sub> O	850	2452	998	1862	1745	862	2177	987	1610	1469
H <sub>2</sub> O	856	2434	1006	1857	1742	861	2080	988	1743	1493

**Table S4.** Comparison of KR-1,<sup>5</sup> KeTMR, and KeJuR

Dye	Solvent	Abs (nm)	Em (nm)	$\epsilon$ ( $M^{-1}\cdot cm^{-1}$ )	$\phi$	$\epsilon \times \phi$ ( $M^{-1}\cdot cm^{-1}$ )	$\tau$ (ns)	Reference
KR-1 / KeTMR	CH <sub>2</sub> Cl <sub>2</sub>	855	911	28400	0.013	369	0.346	Daly et al. <sup>5</sup>
KeTMR	CH <sub>2</sub> Cl <sub>2</sub>	846	882	60700	0.013	789	0.222	This work (KeTMR)
KeJuR	CH <sub>2</sub> Cl <sub>2</sub>	856	883	48600	0.023	1118	0.341	This work (KeJuR)
KR-1 / KeTMR	PBS <sup>a</sup>	862	1058	16500	0.00013	2.15	-	Daly et al. <sup>5</sup>
KeTMR	DPBS <sup>b</sup>	856	1006	26880	0.00013	3.5	-	This work (KeTMR)
KeJuR	DPBS <sup>b</sup>	861	988	21000	0.00032	6.72	-	This work (KeJuR)

<sup>a</sup>PBS: phosphate buffered saline, pH 7.4, containing (in mM): KH<sub>2</sub>PO<sub>4</sub>, 1.06; NaCl, 155.17; Na<sub>2</sub>HPO<sub>4</sub>, 2.97.

<sup>b</sup>DPBS: Dulbecco's phosphate buffered saline, pH 7.2, containing (in mM): KCl, 2.67; KH<sub>2</sub>PO<sub>4</sub>, 1.47; NaCl, 137.93, Na<sub>2</sub>HPO<sub>4</sub>, 8.06.

## Supporting Figures

**Figure S1.** Structures and optical spectra of various tetramethyl xanthene dyes.

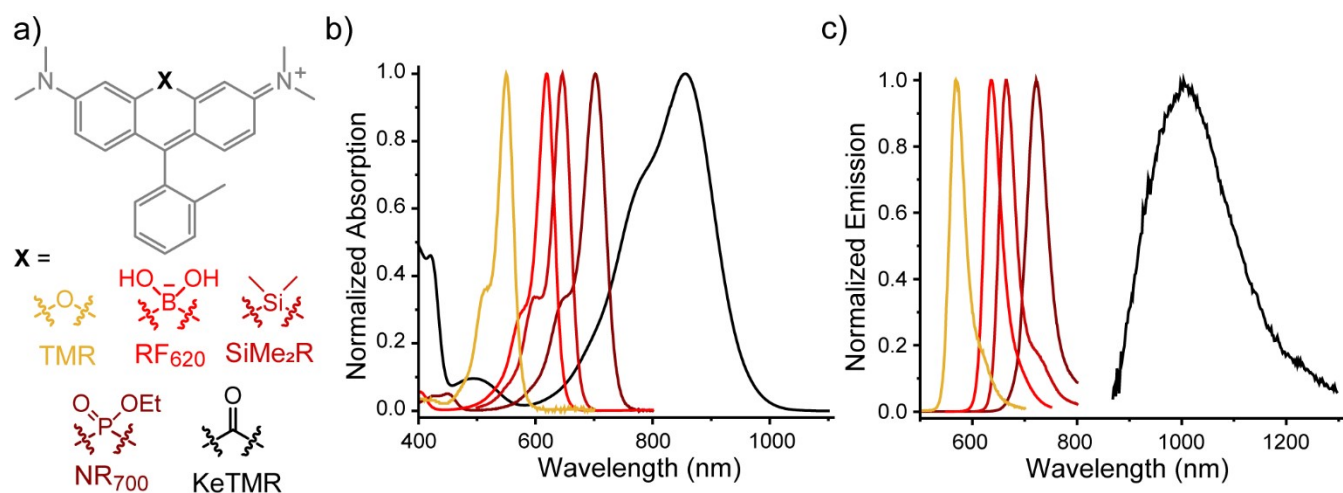


**Figure S1.** Structures and optical spectra of various tetramethyl xanthene dyes. (a) Chemical structures of tetramethyl xanthene dyes bearing different functional groups at 10' position. Normalized absorbance (b) and emission (c) spectra of tetramethyl xanthene dyes under physiological conditions (DPBS, pH=7.2, with 0.5 % DMSO). (Spectrum colors in panel b and c match with the color of structures in panel a.)



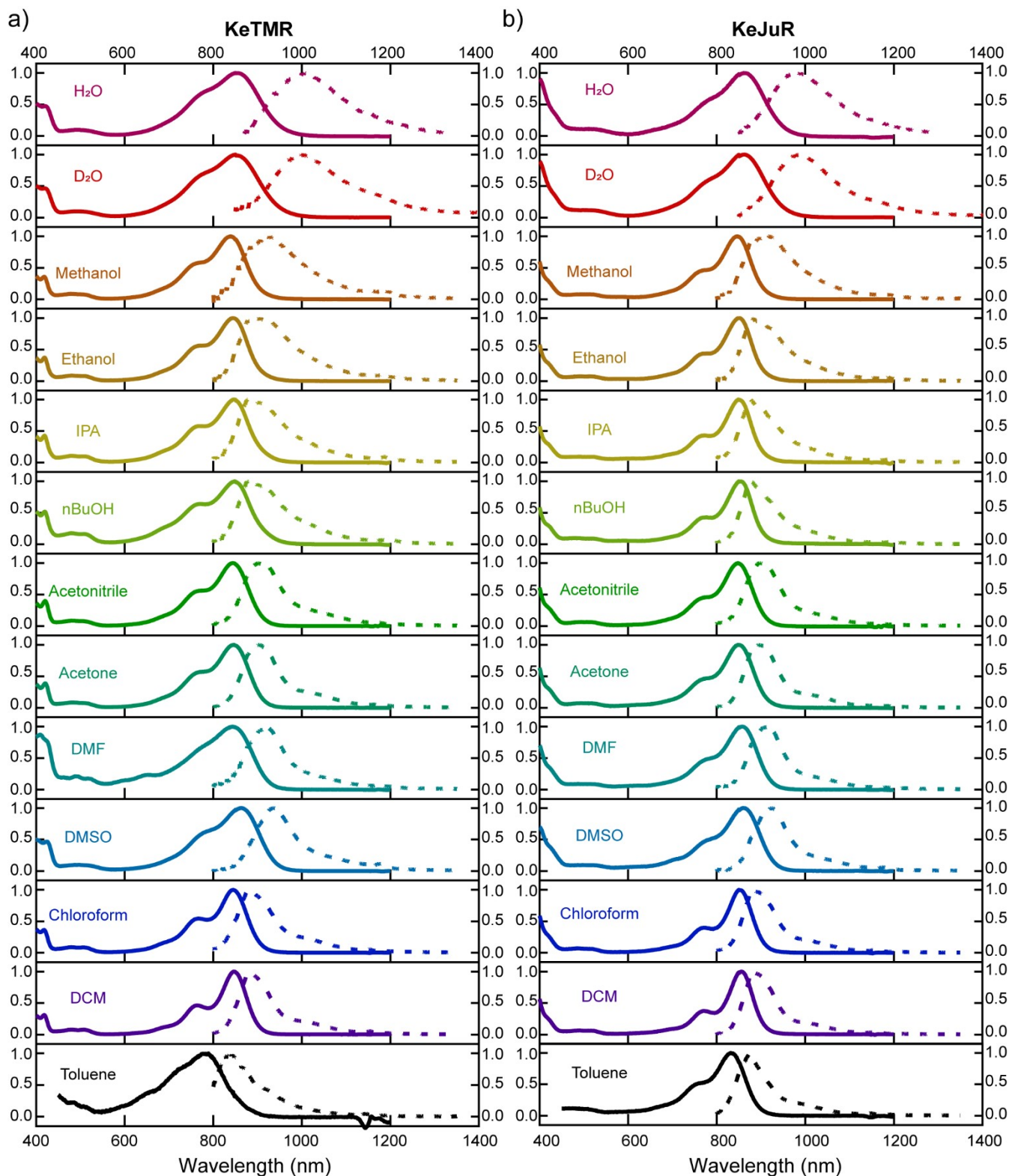
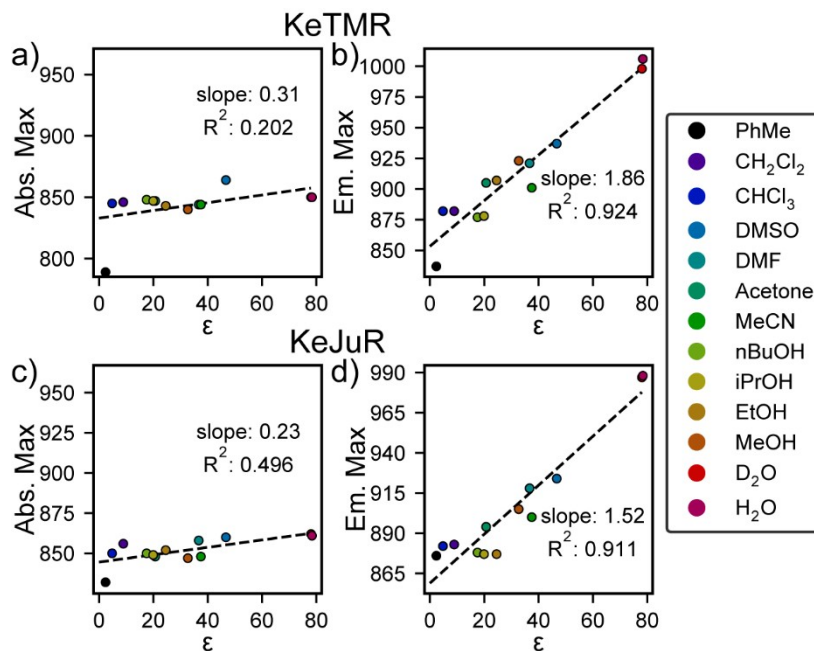


**Figure S2.** Normalized absorbance and fluorescence spectra of KeTMR and KeJuR in various solvents.

**Figure S2.** Normalized absorbance (solid line) and fluorescence (dashed line) spectra of (a) KeTMR and (b) KeJuR in various solvents.



**Figure S3.** The absorption and emission maximum of KeTMR and KeJuR in various solvents against solvent



dielectric constants.

**Figure S3.** The absorption and emission maximum of KeTMR and KeJuR in various solvents were plotted against solvent dielectric constants. Linear fits were applied to these data points. A generally better fit was found for emission than absorption, indicating stronger solvent – excited state dye interaction. A higher slope of KeTMR (1.86) compared to KeJuR (1.52) provided evidence that ketone group is more shielded away from solvent in KeJuR. Panels (b) and (d) are duplicated from the main text (Figure 3b and 4b, respectively) for comparison purposes.

**Figure S4.** Effect of solvent properties on KeTMR and KeJuR

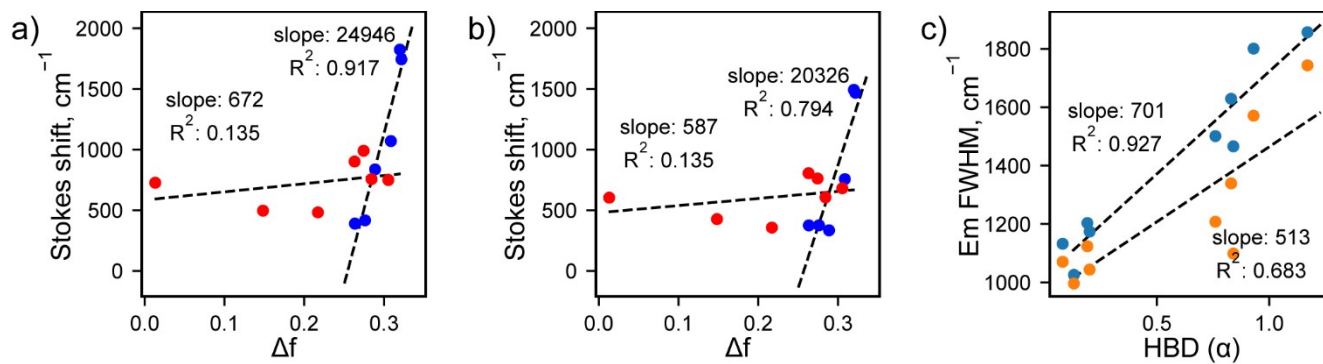


**Figure S4.** Effect of solvent properties on KeTMR and KeJuR. Plots of Stokes shift vs. solvent orientation polarizability ( $\Delta f$ ) (Lippert-Mataga plot)<sup>6</sup> for **a)** KeTMR and **b)** KeJuR. Protic solvents are listed in blue; aprotic solvents are listed in red. **c)** Plot of the emission full width at half-maximum (FWHM) for KeTMR (blue) and KeJuR (orange) vs. hydrogen bond donation strength (HBD) alpha ( $\alpha$ ) values. Dashed line is the line of best fit. HBD values are from Kamlet, *et al.*<sup>7</sup>

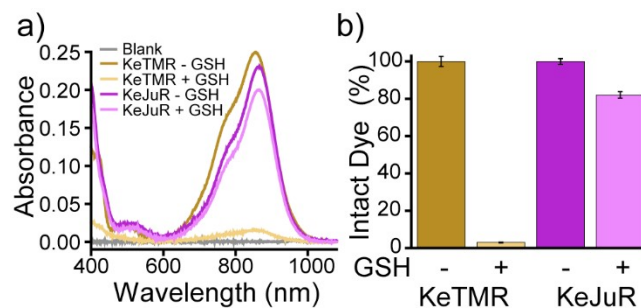


**Figure S5.** KeTMR and KeJuR chemical stabilities against GSH.

**Figure S5.** Chemical stabilities of KeTMR and KeJuR against GSH. 20  $\mu\text{M}$  dyes were added into freshly made 2 mM GSH solution in DPBS (pH = 7.2), and react at room temperature for 45 min. After measuring the blank (2 mM GSH in DPBS), same volume of reaction mixture was added so the theoretical dye concentration was 10  $\mu\text{M}$ . Intact dye percentage was calculated using the dyes' molar extinction coefficient and the absorbance measured from the reaction mixture. Each condition was repeated three times to get the standard error.

**Figure S6.** KeJuR concentration dependent PA signal.

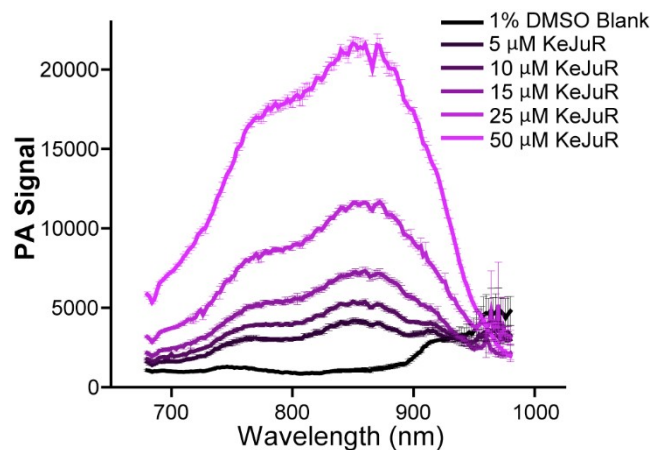


**Figure S6.** KeJuR of various concentrations (5-50  $\mu$ M) were injected into the FEP tube in tissue phantom, and the whole spectra were scanned from 680 nm to 980 nm with 2 nm interval. For each wavelengths, 7 different z positions were scanned and averaged to get the standard error.

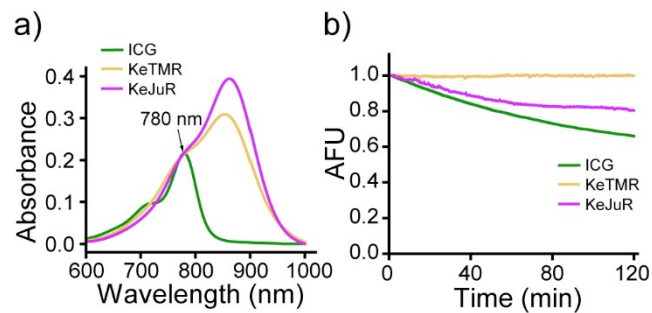
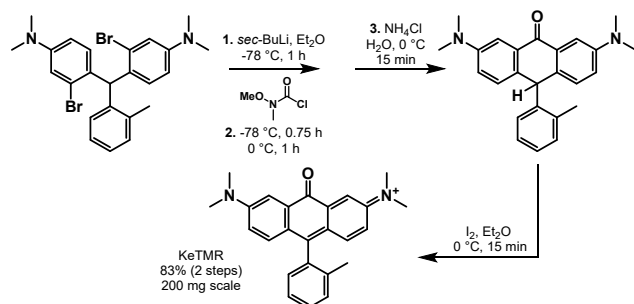


**Figure S7.** Photostability of KeTMR and KeJuR.

**Figure S7.** (a) The absorbance at 780 nm of 3 dyes (ICG, KeTMR and KeJuR) in DPBS (pH = 7.2, with 1 % DMSO) was firstly normalized to 0.215. (b) Fluorescence at each emission maximum was then monitored over 2 hours with the same excitation (780 nm).

## Detailed Synthetic Procedures



### Screening electrophiles for KeTMR synthesis:

To a flame-dried 50 mL Schlenk-flask, 4,4'-(*o*-tolylmethylene)bis(3-bromo-*N,N*-dimethylaniline)<sup>8</sup> (200 mg, 0.4 mmol, 1 eq.) was dissolved in 12 mL anhydrous diethyl ether. Heating and sonication were applied to ensure the complete solubilization of the white solid. The flask was then immersed in a dry ice / acetone bath to lower the temperature to -78 °C. After stirring at this temperature for 5 min, 3 cycles of vacuum and N<sub>2</sub> were applied. After additional 10 min, *sec*-Butyl lithium solution (1.4 M in cyclohexane, 657 μL, 0.92 mmol, 2.3 eq.) was added dropwise into the reaction mixture via a 1 mL syringe with a counter flow of N<sub>2</sub>. The reaction was proceeded at the same temperature in dark for 1 h, before the electrophile (listed in Table S1, 0.48 mmol, 1.2 eq.) dissolved in anhydrous diethyl ether (4 mL) being added dropwise into the reaction mixture. After stirring at -78 °C for additional 45 min, the dry ice / acetone bath was replaced by an ice bath to allow the reaction temperature raise to 0 °C. The reaction was left at this temperature for 1 h, before ice cold ammonium chloride solution (saturated, 10 mL) was carefully added into the mixture. After 15 min, the reaction mixture was poured into a separation funnel and extracted with diethyl ether (3×20 mL). The organic layer was collected and dried with sodium sulfate, and solvent was removed by rotavapor. The resulting yellow to brown solid was dissolved back to diethyl ether (15 mL) and the temperature was lowered to 0 °C. Solid iodine (112 mg, 0.44 mmol, 1.1 eq.) was added in one portion and left at the same temperature for 15 min. The solution became cloudy after 5 min and when the reaction was complete, the brown solid precipitated from the solution was collected via filtration. The dark brown solid was rinsed with additional ether (3×5 mL), and dried under vacuum overnight in the dark. The solid was found to be NMR pure and yields with different electrophiles were summarized in Table S1. For spectroscopic analysis, the KeTMR solid obtained above was further purified with prep HPLC.

While characterizing the KeTMR product via NMR, to our surprise, the lyophilized powder from prep HPLC gave no clear product peaks in <sup>1</sup>H NMR (Spectrum S1), while the one directly obtained from filtration after iodine oxidation gave good NMR. Additionally, we further added solid iodine into the NMR tube containing the HPLC purified KeTMR and the signal could be regenerated again (Spectrum S2). From these observations, we hypothesized that pure KeTMR had radical characterizations in solution, making it NMR silent, and that iodine was acting as a radical scavenger. This hypothesis was confirmed with EPR experiments (Spectrum S3), where clear EPR signal could be seen in KeTMR alone (2 mM in dichloromethane, from HPLC purified), while the addition of solid iodine quenched the EPR signal to baseline, similar to blank solvent (dichloromethane only).

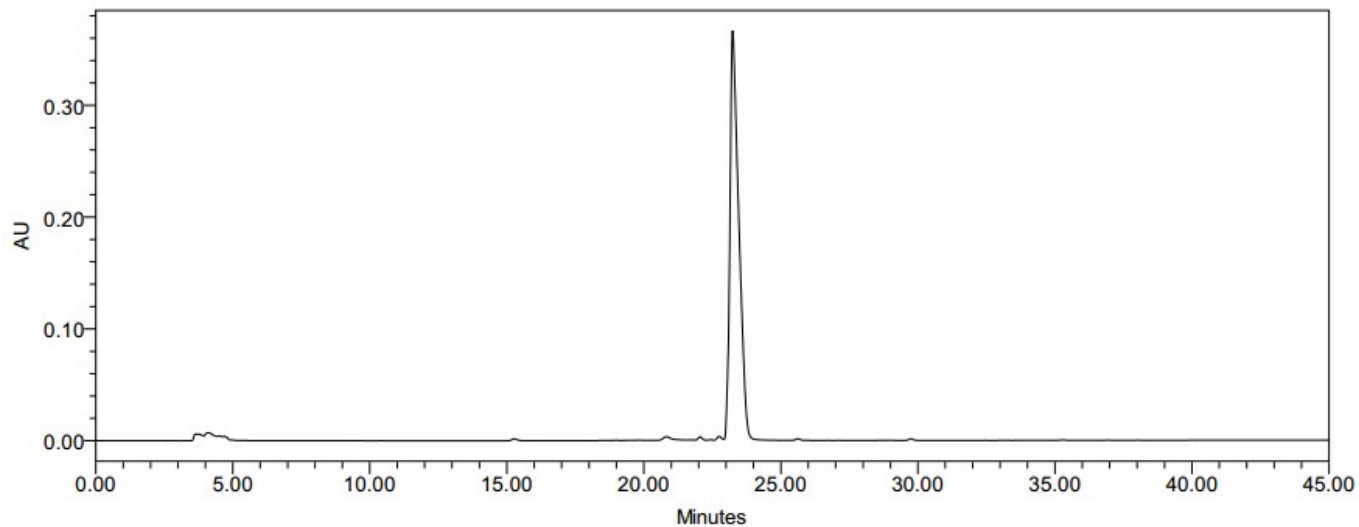
<sup>1</sup>H NMR (600 MHz, Chloroform-*d*) δ 7.81 (d, *J* = 2.8 Hz, 2H), 7.49 – 7.44 (m, 1H), 7.38 (t, *J* = 7.5 Hz, 2H), 7.23 (s, 1H), 7.02 (d, *J* = 9.3 Hz, 2H), 6.76 (dd, *J* = 9.3, 2.8 Hz, 2H), 3.48 (s, 12H), 2.18 (s, 3H).

<sup>13</sup>C NMR (151 MHz, Chloroform-*d*) δ 183.42, 165.66, 156.95, 138.76, 136.31, 135.42, 133.87, 130.83, 129.97, 129.20, 126.16, 124.46, 117.12, 116.20, 77.37, 77.16, 76.95, 42.34, 20.29.

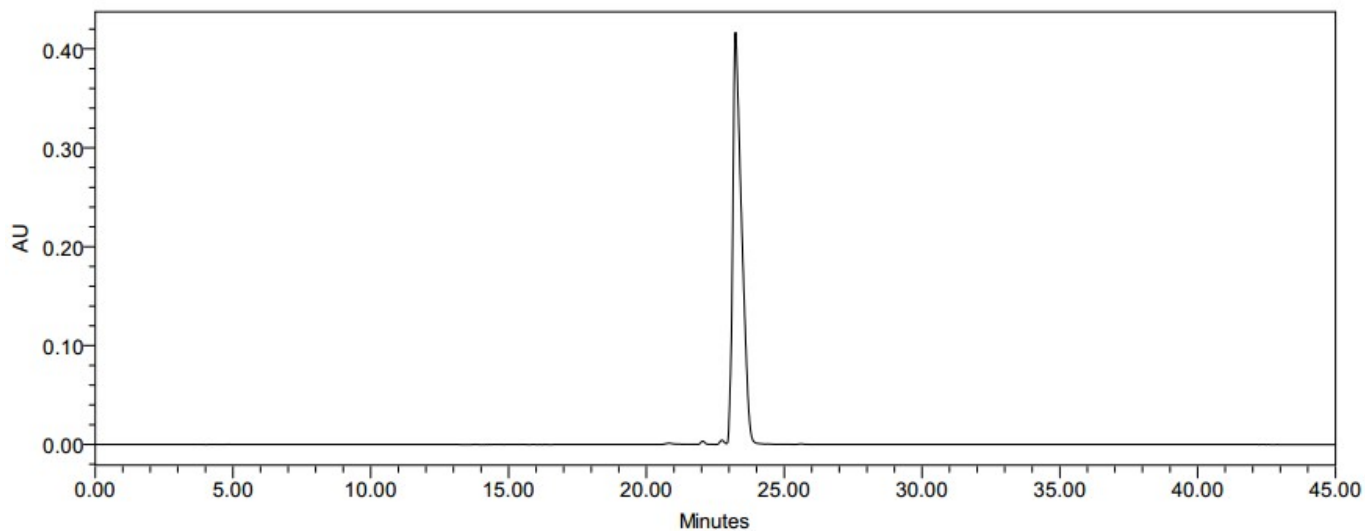
HR-ESI-MS *m/z* for C<sub>25</sub>H<sub>25</sub>N<sub>2</sub>O<sup>+</sup> [M]<sup>+</sup> calcd: 369.1961 found: 369.2008 (+4.7 ppm)



HPLC purity check of KeTMR (@ 254 nm).



HPLC purity check of KeTMR (@ 280 nm).

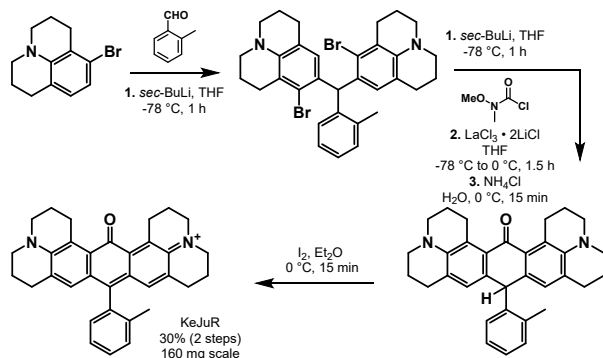


HPLC buffer A: 99.9 % water + 0.1 % trifluoroacetic acid.

HPLC buffer B: 99.9 % acetonitrile + 0.1 % trifluoroacetic acid.

Method: 95 % A (0 – 1 min), 95 % A to 75 % A (1 min – 5 min), 75 % A to 0 % A (5 min – 40 min), 0 % A (40 min – 44 min), and 0% to 95 % A (44 – 45 min).

## Synthesis of KeJuR



### Synthesis of 9,9'-(*o*-tolylmethylene)bis(8-bromo-2,3,6,7-tetrahydro-1*H*,5*H*-pyrido[3,2,1-*ij*]quinoline)

8-bromo-2,3,6,7-tetrahydro-1*H*,5*H*-pyrido[3,2,1-*ij*]quinoline<sup>8</sup> (10 g, 39.66 mmol, 4 eq.), *p*-toluenesulfonic acid monohydrate (1.886 g, 9.91 mmol, 1 eq.) were dissolved in 50 mL toluene in a 100 mL round bottom flask. After vacuum and recharging the flask with  $\text{N}_2$  three times, *o*-Tolualdehyde (1.146 mL, 9.91 mmol, 1 eq.) was added and the reaction was refluxed using a Dean-Stark apparatus for 3 hours. The flask was then removed from the oil bath, and once the mixture reached ambient temperature, excess toluene was removed by rotavapor. The mixture was further dissolved in ethyl acetate and washed with sodium bicarbonate solution. Organic layer was collected and dried with sodium sulfate and solvent was removed by rotavapor. Flash column chromatography (1 % - 8 % ethyl acetate in hexane) gave the product as a white solid (2.38 g, 3.92 mmol, 40 %).

<sup>1</sup>H NMR (600 MHz, Chloroform-*d*)  $\delta$  7.13 – 7.02 (m, 3H), 6.74 (d,  $J = 7.5$  Hz, 1H), 6.23 (s, 2H), 6.02 (s, 1H), 3.20 – 2.97 (m, 8H), 2.79 (t,  $J = 6.7$  Hz, 4H), 2.58 (tt,  $J = 16.2, 8.1$  Hz, 4H), 2.20 (s, 3H), 2.07 – 1.80 (m, 8H).

<sup>13</sup>C NMR (151 MHz, Chloroform-*d*)  $\delta$  142.97, 142.57, 137.27, 130.06, 129.80, 129.00, 128.98, 126.70, 125.95, 125.44, 121.41, 120.14, 53.06, 50.24, 49.71, 29.64, 27.78, 22.43, 22.10, 19.86.

ESI-MS  $m/z$  for  $\text{C}_{32}\text{H}_{35}\text{Br}_2\text{N}_2^+$   $[\text{M}+\text{H}]^+$  calcd: 605.1162 found: 605.1129 (-5.45 ppm).

## Synthesis of KeJuR

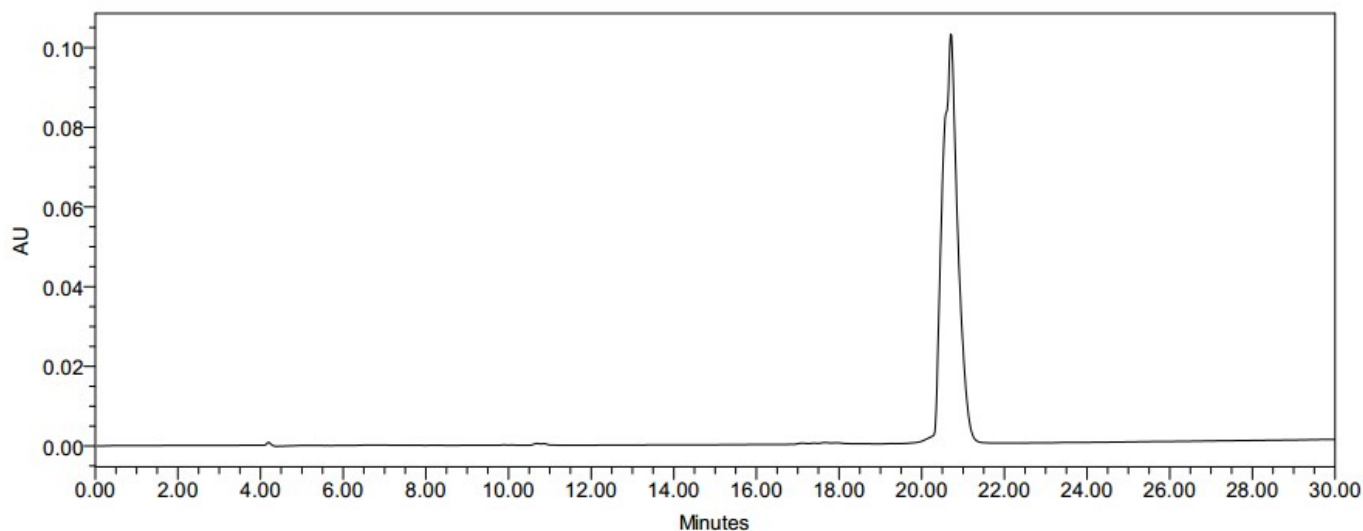
To a flame dried 50 mL Schlenk flask, 9,9'-(*o*-tolylmethylene)bis(8-bromo-2,3,6,7-tetrahydro-1*H*,5*H*-pyrido[3,2,1-*ij*]quinoline) (160 mg, 0.264 mmol, 1 eq.) was dissolved in anhydrous tetrahydrofuran (THF, 6 mL). The mixture temperature was lowered to -78 °C with a dry ice / acetone bath and maintained for 15 min. After three cycles of vacuum and N<sub>2</sub>, *sec*-butyl lithium solution (1.4 M in cyclohexane, 792 μL, 1.109 mmol, 4.2 eq.) was added dropwise into the reaction mixture via a 1 mL syringe with a counter flow of N<sub>2</sub>. The reaction was left at the same temperature in the dark for 1 h, before LaCl<sub>3</sub>·2LiCl (0.6 M in THF, 968 μL, 0.581 mmol, 2.2 eq.) was added at the same temperature. The solution color turned from orange to light yellow over 30 min. *N*-Methoxy-*N*-methylcarbamoyl chloride (40 μL, 0.396 mmol, 1.5 eq.) dissolved in anhydrous THF (3 mL) was then injected into the reaction at -78 °C and maintained for 15 min. The dry ice / acetone bath was then replaced with an ice bath and the mixture was stirred at 0 °C for 90 min. Ice cold ammonium chloride solution (saturated, 10 mL) was carefully added into the reaction. After 15 min, the reaction mixture was poured into a separation funnel and extracted with diethyl ether (3×20 mL). The organic layer was collected and dried with sodium sulfate, and solvent was removed by rotavapor. The brown solid was re-dissolved back in diethyl ether (15 mL) and the temperature was lowered to 0 °C. Solid iodine (74 mg, 0.29 mmol, 1.1 eq.) was added in one portion and the mixture was stirred at 0 °C for 15 min. The dark brown precipitates were filtered and further purified by HPLC to yield KeJuR as a brown solid (47 mg, 0.08 mmol, 30 %).

Unlike KeTMR, we were able to get clean NMR spectra for KeJuR after the HPLC purification. The dye stock solution (10 mM in DMSO) was found to be unstable, even stored in -80 °C in the dark. From the LC-MS trace of the impurities, oxidation reaction was suspected to occur on the julolidine rings. As a result, dyes were made to 10 mM in acetonitrile / water (1:1, v:v) and aliquoted into small vials and lyophilized to powder form. The storage of this solid form of KeJuR was found to be stable for at least 6 months in -80 °C in the dark. Same volume of solvents was added back into the vial, immediately before usage.

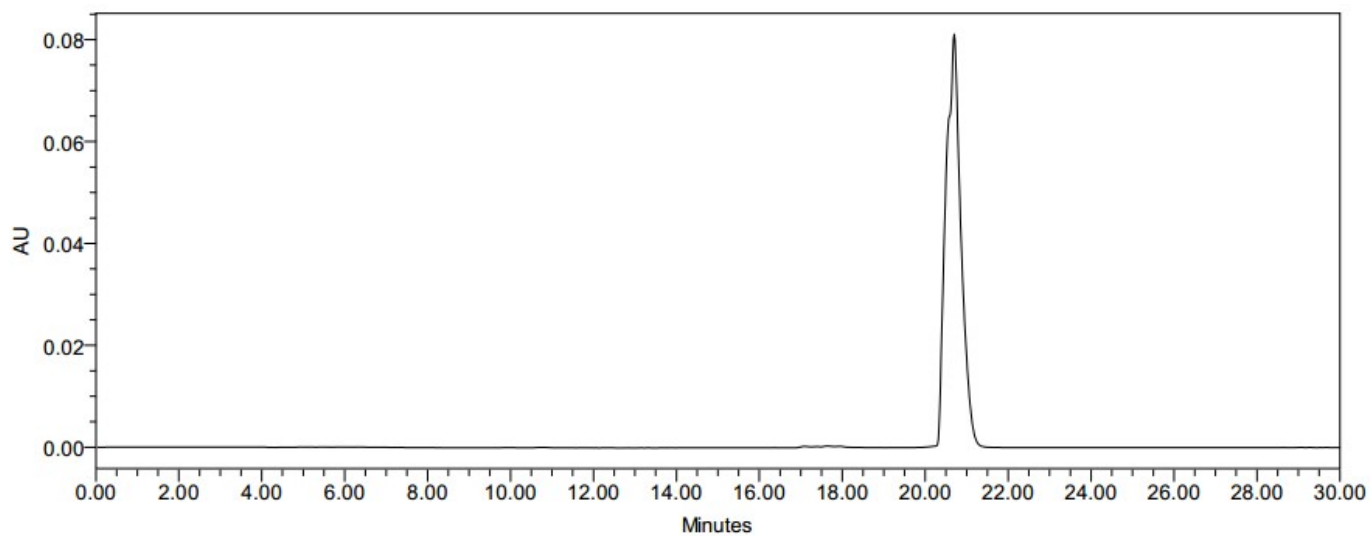
<sup>1</sup>H NMR (600 MHz, Chloroform-*d*) δ 7.44 (td, *J* = 7.5, 1.3 Hz, 1H), 7.35 (dd, *J* = 14.0, 7.4 Hz, 2H), 7.07 (dd, *J* = 7.5, 1.3 Hz, 1H), 6.40 (s, 2H), 3.58 (q, *J* = 4.9 Hz, 8H), 3.30 – 3.18 (m, 4H), 2.62 – 2.49 (m, 4H), 2.09 (s, 3H), 2.03 (p, *J* = 7.5 Hz, 4H), 1.94 (p, *J* = 6.1 Hz, 4H).

<sup>13</sup>C NMR (151 MHz, Chloroform-*d*) δ 190.16, 160.67, 152.36, 136.11, 134.73, 133.79, 133.38, 130.92, 130.42, 129.28, 129.25, 125.83, 124.61, 123.71, 52.48, 51.37, 27.50, 26.07, 20.55, 20.26, 19.62.

HR-ESI-MS *m/z* for C<sub>33</sub>H<sub>33</sub>N<sub>2</sub>O<sup>+</sup> [*M*]<sup>+</sup> calcd: 473.2587 found: 473.2610 (+4.86 ppm)



HPLC purity check of KeJuR (@ 254 nm).



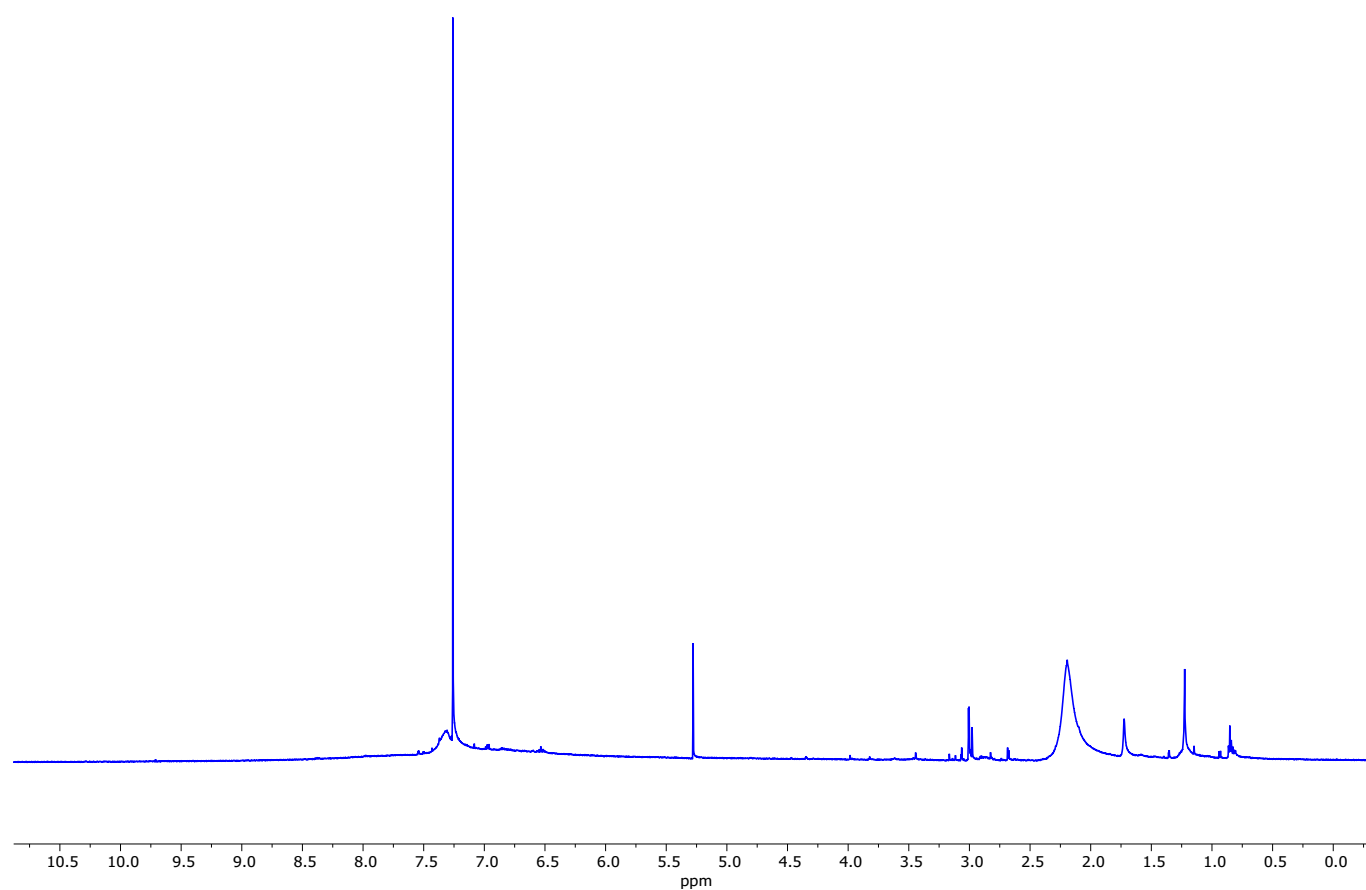
HPLC purity check of KeJuR (@ 365 nm).

HPLC buffer A: 99.9 % water + 0.1 % trifluoroacetic acid.

HPLC buffer B: 99.9 % acetonitrile + 0.1 % trifluoroacetic acid.

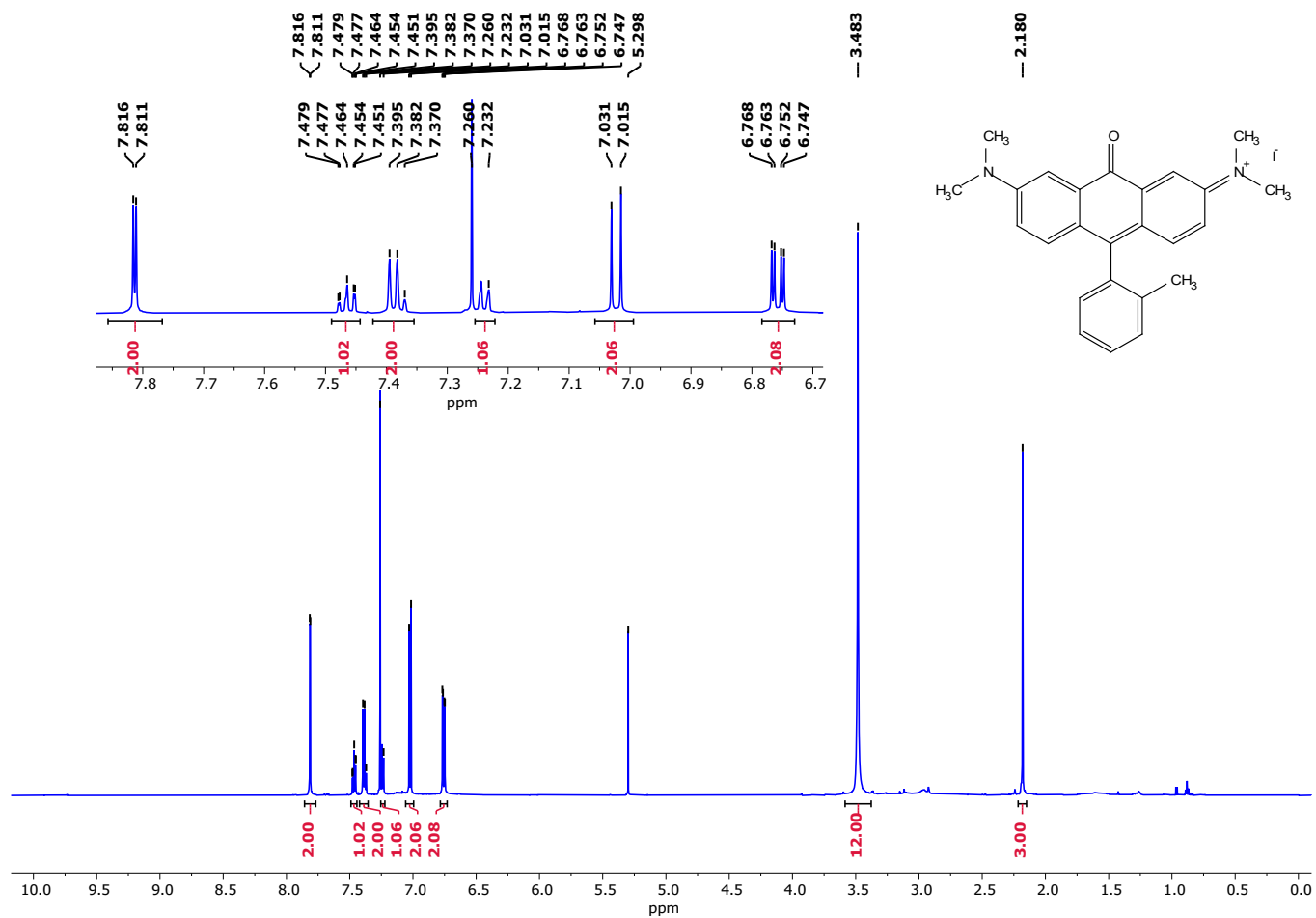
Method: 95 % A (0 – 1 min), 95 % A to 60 % A (1 min – 5 min), 60 % A to 0 % A (5 min – 25 min), 0 % A (25 min – 29 min), and 0% to 95 % A (29 – 30 min).

## Supporting Spectra

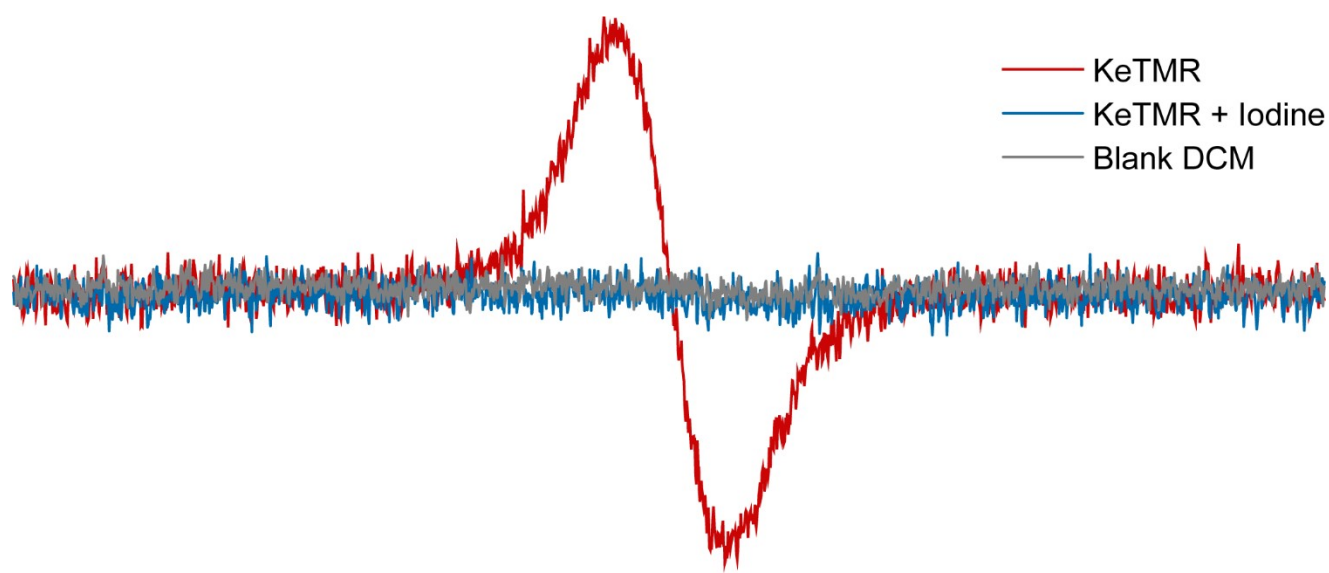


**Spectrum S1.** <sup>1</sup>H NMR chart of KeTMR without I<sub>2</sub> in Chloroform-*d*. No clear product peaks could be assigned.

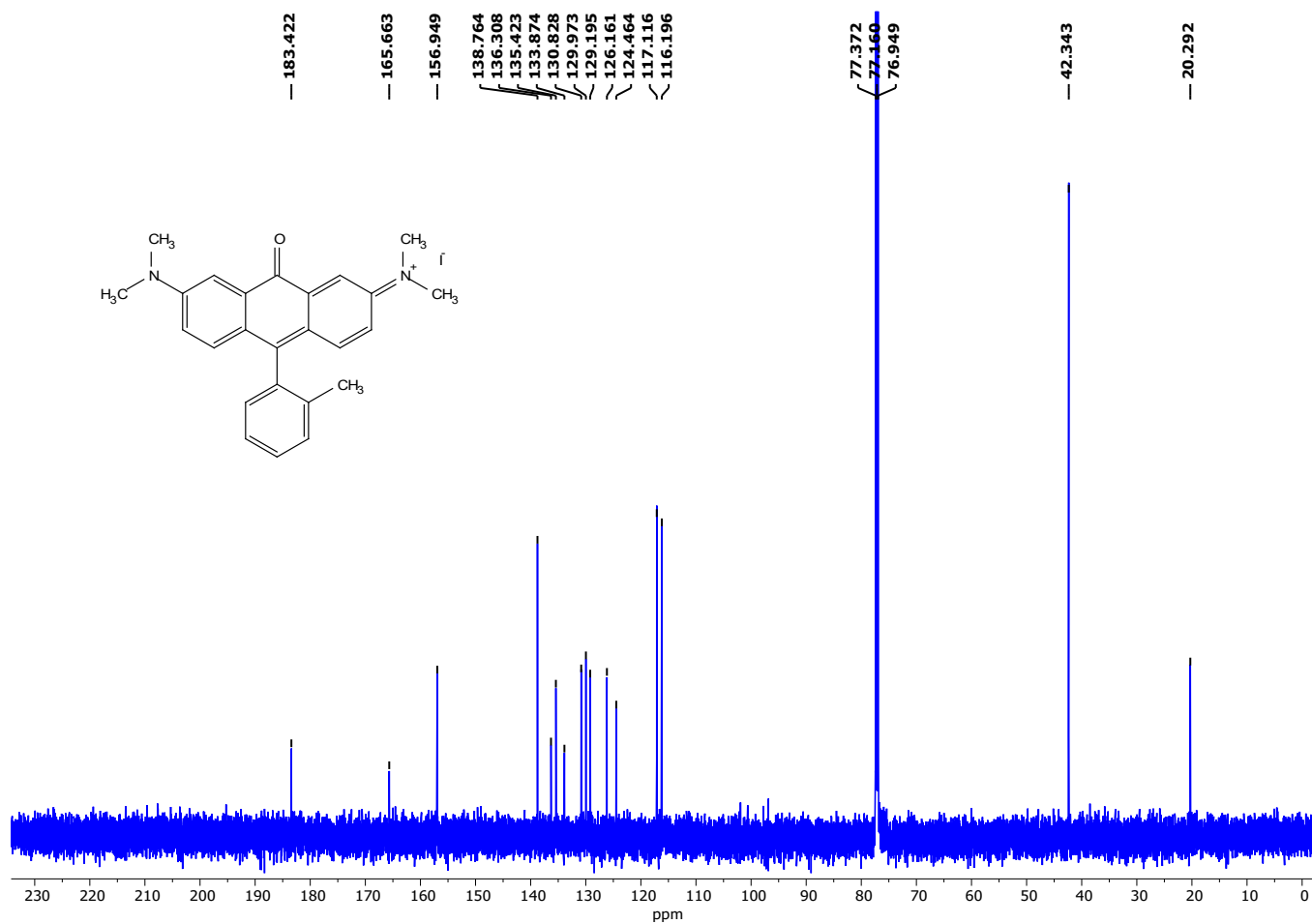
Spectrum S2. <sup>1</sup>H NMR chart of KeTMR with I<sub>2</sub> in Chloroform-*d*.



**Spectrum S3.** EPR Spectrum of KeTMR (2 mM in Dichloromethane) with and without Iodine.

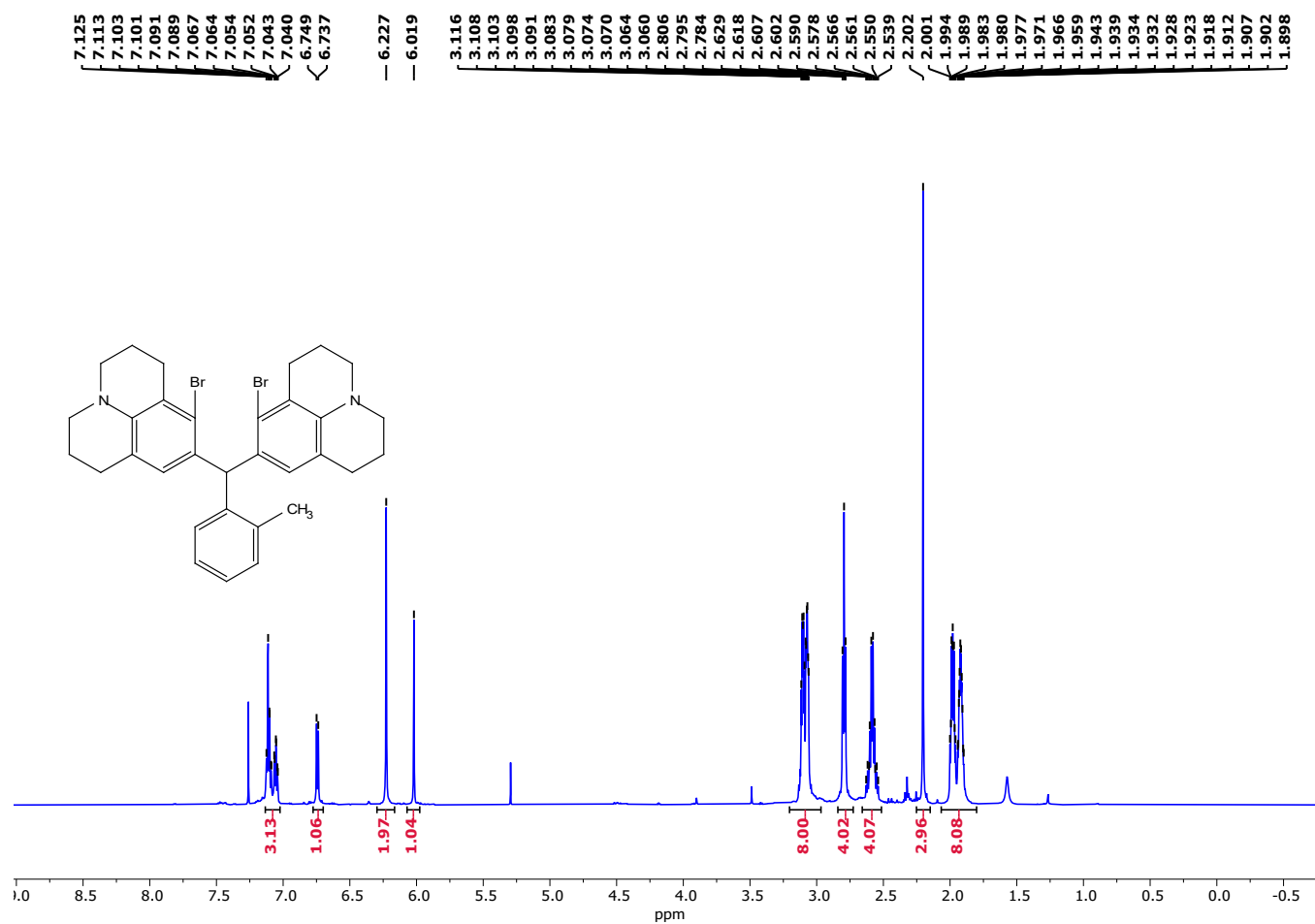


Spectrum S4. <sup>13</sup>C NMR chart of KeTMR with I<sub>2</sub> in Chloroform-*d*.

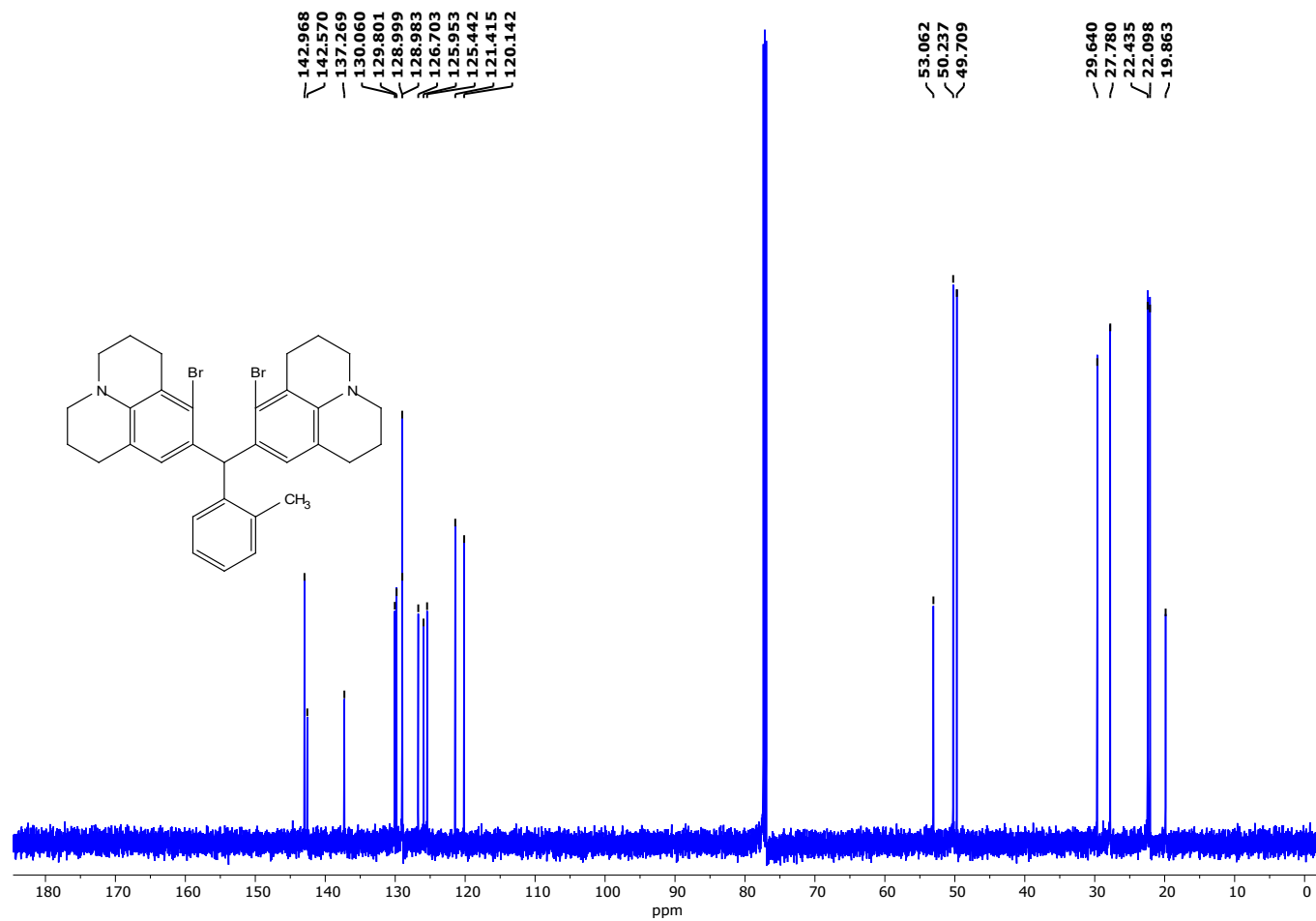




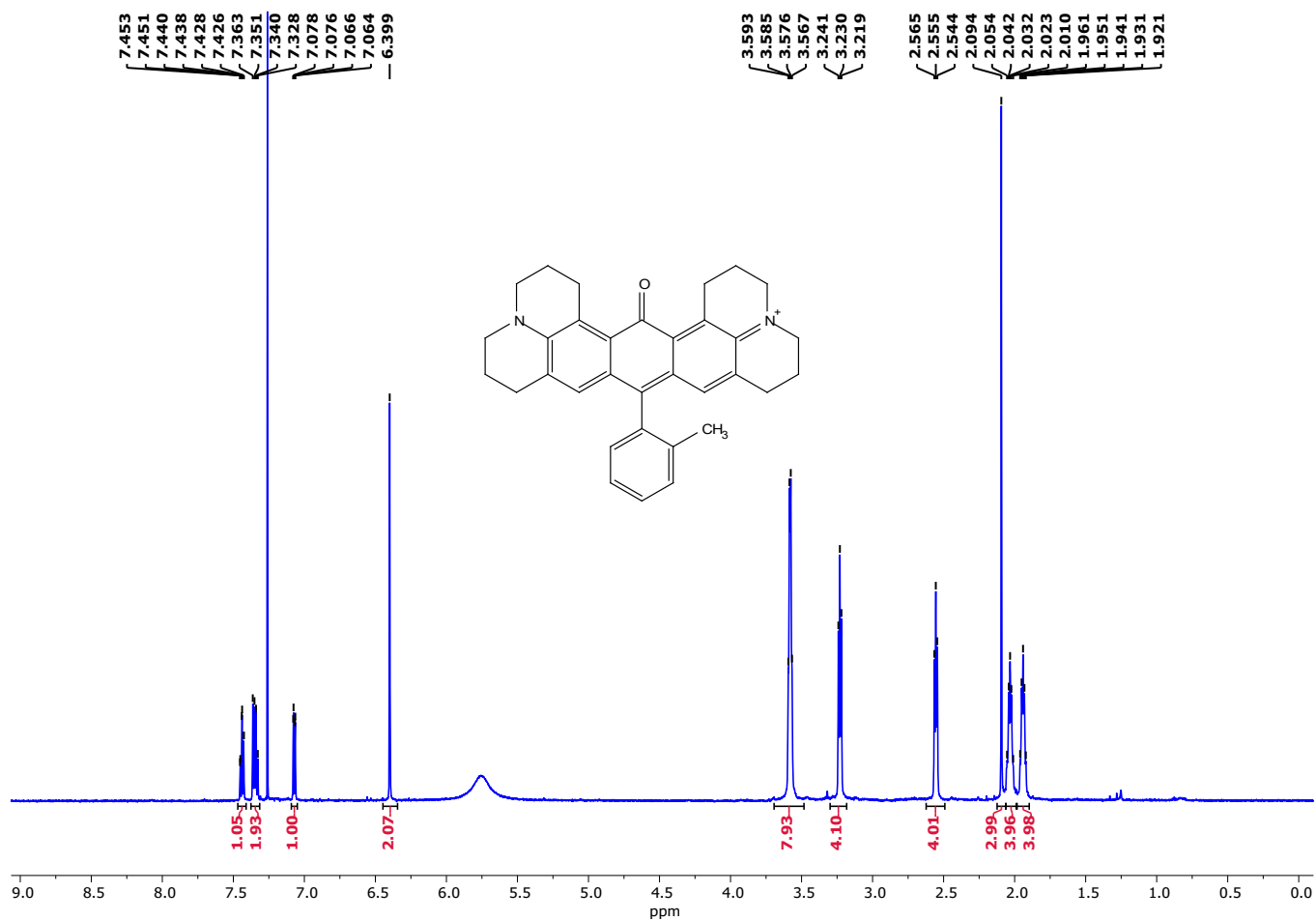
**Spectrum S5.**  $^1\text{H}$  NMR chart of 9,9'-(*o*-tolylmethylene)bis(8-bromo-2,3,6,7-tetrahydro-1H,5H-pyrido[3,2,1-ij]quinoline) in Chloroform-*d*.



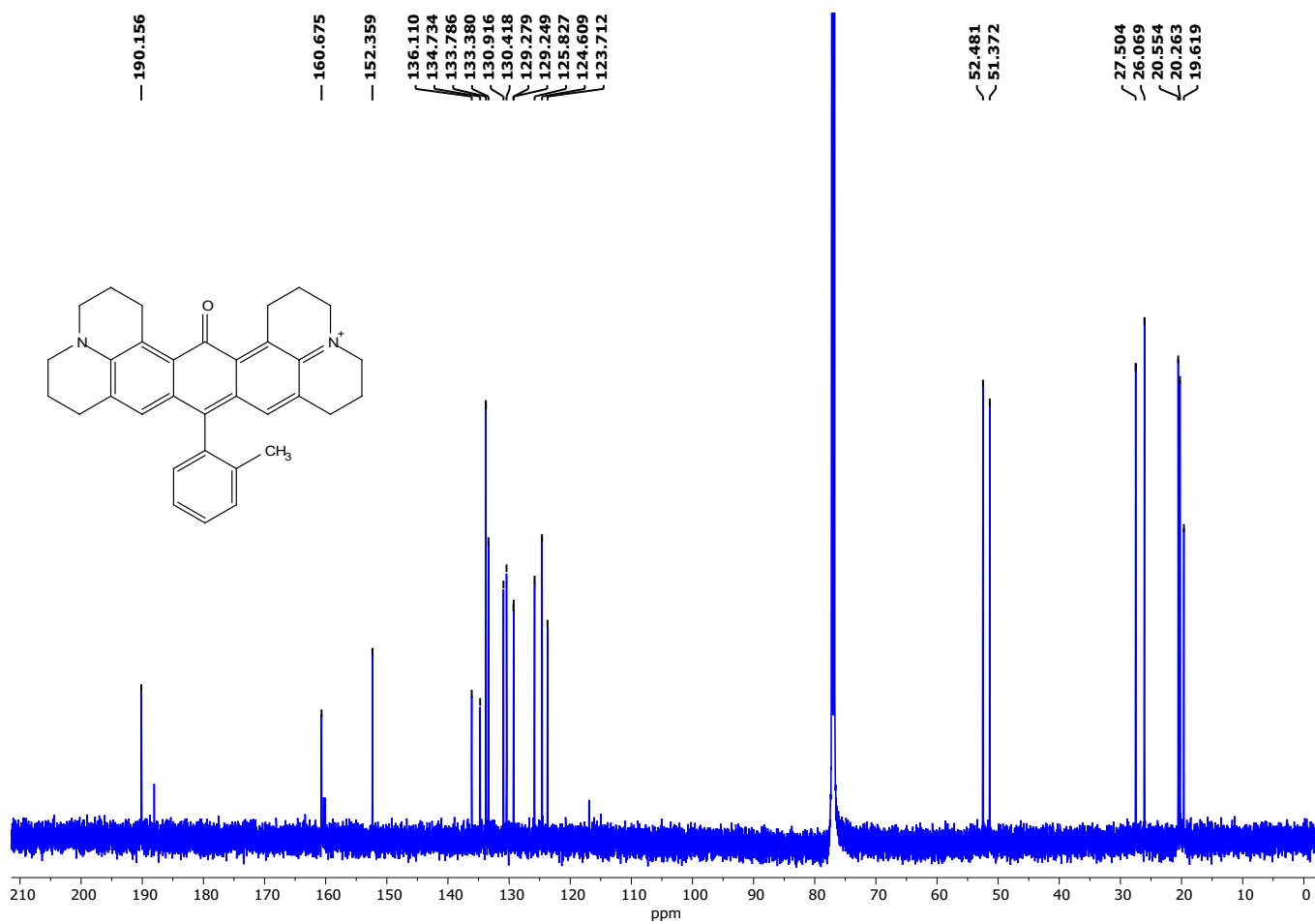
**Spectrum S6.**  $^{13}\text{C}$  NMR chart of 9,9'-(*o*-tolylmethylene)bis(8-bromo-2,3,6,7-tetrahydro-1H,5H-pyrido[3,2,1-ij]quinoline) in Chloroform-*d*.



Spectrum S7. <sup>1</sup>H NMR chart of KeJuR in Chloroform-d.



Spectrum S8. <sup>13</sup>C NMR chart of KeJuR in Chloroform-*d*.



## References

1. D. Bradley, G. Williams and M. Lawton, *J Org Chem*, 2010, **75**, 8351-8354.
2. R. Dulbecco and M. Vogt, *The Journal of experimental medicine*, 1954, **99**, 167-182.
3. R. Hoshi, K. Suzuki, N. Hasebe, T. Yoshihara and S. Tobita, *Anal Chem*, 2020, **92**, 607-611.
4. H. J. Knox, J. Hedhli, T. W. Kim, K. Khalili, L. W. Dobrucki and J. Chan, *Nat Commun*, 2017, **8**.
5. H. C. Daly, S. S. Matikonda, H. C. Steffens, B. Ruehle, U. Resch-Genger, J. Ivanic and M. J. Schnermann, *Photochem Photobiol*, 2022, **98**, 325-333.
6. M. Noboru, K. Yozo and K. Masao, *Bull Chem Soc Jpn*, 1956, **29**, 465-470.
7. M. J. Kamlet, J. L. M. Abboud, M. H. Abraham and R. W. Taft, *J Org Chem*, 1983, **48**, 2877-2887.
8. X. Q. Zhou, R. Lai, J. R. Beck, H. Li and C. I. Stains, *Chem Commun*, 2016, **52**, 12290-12293.